

Numerical evaluation of FRP composite retrofitted reinforced concrete wall subjected to blast load

Jin-Won Nam^{*1}, In-Seok Yoon^{2a} and Seong-Tae Yi^{3b}

¹Baytech Korea Inc., 8F, 464 Dunchon-Daero, Jungwon-gu, Seongnam-si, Gyeonggi-do, 13229, Korea

²Department of Construction Information Engineering, Induk University, 12 Choansan-ro, Nowon-gu, Seoul, 01880, Korea

³Department of Civil & Environmental Engineering, Inha College, 100 Inha-Ro, Nam-Gu, Incheon, 22212, Korea

(Received October 5, 2015, Revised December 1, 2015, Accepted December 10, 2015)

Abstract. High performance materials such as Fiber Reinforced Plastic (FRP) are often used for retrofitting structures against blast loads due to its ductility and strength. The effectiveness of retrofit materials needs to be precisely evaluated for the retrofitting design based on the dynamic material responses under blast loads. In this study, the blast resistance of Carbon Fiber Reinforced Plastic (CFRP) and Kevlar/Glass hybrid fabric (K/G) retrofitted reinforced concrete (RC) wall is analyzed by using the explicit analysis code LS-DYNA, which accommodates the high-strain rate dependent material models. Also, the retrofit effectiveness of FRP fabrics is evaluated by comparing the analysis results for non-retrofitted and retrofitted walls. The verification of the analysis is performed through comparisons with the previous experimental results.

Keywords: HFPB analysis; blast resistance; FRP Composite; strain rate; LS-DYNA

1. Introduction

Generally, concrete can be considered as a highly effective construction material in resisting against blast loading compared to other materials. However, concrete structures designed for the service loads of normal strain rate require special retrofitting to increase the structural resistance against blast loading. Retrofitting method of attaching extra structural members or supports to increase the blast resistance is undesirable from the perspectives of construction cost increase and useable space elimination. Also, this method generally does not greatly improve the overall structural resistance against blast load (ASCE 1999). Therefore, less expensive and more convenient fiber reinforced polymers (FRP) sheets or plates are being used as surface attachments to retrofit specified areas of structural members (Buchan and Chen 2007, Brena and McGuirk 2013, Grelle and Sneed 2013). The FRP surface attachments significantly improve the blast resistance of structures without forfeiting usable space and requiring long construction time,

*Corresponding author, Ph.D., E-mail: jwnam72@gmail.com

^aProfessor, E-mail: isyoon@induk.ac.kr

^bProfessor, E-mail: yist@inhac.ac.kr

thereby saving money. For the retrofitting of concrete structures for blast resistance, the selection of the type of FRP is important. The selected FRP has to improve stiffness, strength, and ductility of a retrofitted structure to satisfy required blast safety resistance and absorb blast energy whereby transforming structural failure mode from brittle to ductile.

To analyze and design FRP retrofitted structures under blast loads, both experimental and numerical studies are necessary (Muszynski and Purcell 2003, White *et al.* 2001, Jerome and Ross 1997, Silva and Lu 2007). Simplified lumped mass models for blast resistant structure design and analysis allow rudimentary ways of designing and analyzing global concrete structure displacement behavior in terms of applied load, mass, and resistance factors (Biggs 1964). In such methods, the applied load is calculated based on the application of simple blast wave function and conversion of overall structural stiffness to a single stiffness value. Due to its simplicity, this method is still commonly used for blast resistant structure design and analysis. However, recently, in order to improve the simplified analysis methods, studies on the precise blast analysis methods with accurate material models and refined finite element models for the simulation of retrofitted concrete structure behavior have been actively pursued for the accuracy and reliability of analysis results (Malvar *et al.* 2004, Razaqpur and Tolba 2007).

If properly validated, the refined FEM analyses can be used as a replacement for costly structure blast experiments. Furthermore, even when specialized testing facilities and related resources are available, some conditions and data are more readily obtained through such virtual experiments using the FEM. For these reasons, it is vital to establish effective analysis tools for new and retrofitted concrete structures under blast loading to predict structural behaviors, select optimum retrofit materials, and ensure desired failure mechanisms.

In this study, the blast resistance of Carbon Fiber Reinforced Plastic (CFRP) and Kevlar/Glass hybrid fabric (K/G) retrofitted reinforced concrete (RC) wall is analyzed by using the explicit analysis code LS-DYNA, which accommodates the high-strain rate dependent material models. Also, the retrofit effectiveness of FRP fabrics is evaluated by comparing the analysis results for non-retrofitted and retrofitted walls. The verification of the analysis is performed through comparisons with experimental results.

2. Constitutive material models

2.1 Rate dependent concrete damage model

The concrete damage model used in this study is based on Malvar's model (2004), which modifies the Willam-Warnke failure surface with three parameter surface definition and pressure cutoff (Chen 1982). The concrete damage model of this study represents blast dynamic hardening-softening nonlinear behavior by accumulated effective plastic strain in the regime of continuum mechanics. In the model, three independent failure surfaces are defined as

$$\Delta\sigma_m = a_0 + \frac{\rho}{a_1 + a_2\rho} \quad (\text{Maximum failure surface}) \quad (1)$$

$$\Delta\sigma_r = \frac{\rho}{a_{1f} + a_{2f}\rho} \quad (\text{Residual failure surface}) \quad (2)$$

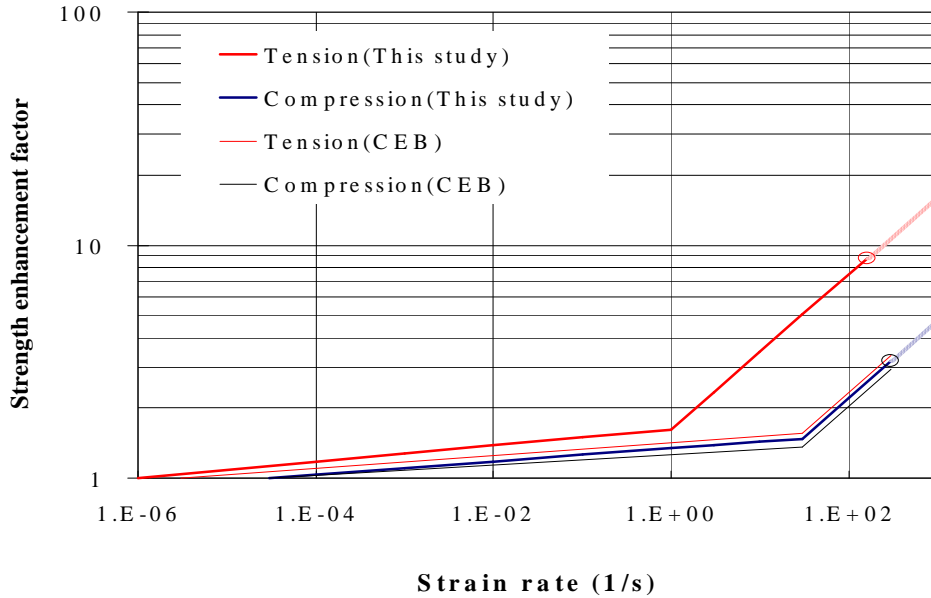


Fig. 1 Concrete strength enhancement due to high strain rates

$$\Delta\sigma_y = a_{0y} + \frac{p}{a_{1y} + a_{2y}p} \quad (\text{Yield failure surface}) \quad (3)$$

$$\Delta\sigma_e = r_f \Delta\sigma(p/r_f) \quad (\text{Enhanced failure surface}) \quad (4)$$

where, $\Delta\sigma$ is stress difference (on the deviatoric stress failure surface) and p is confining pressure for each stage of behavior. The variables a_0 , a_1 , and a_2 are constants obtained by the unconfined compression test and conventional triaxial compression tests at various degrees of confining pressure. r_f is the strength enhancement factor, which represents strain rate effect of concrete. The enhanced concrete strength is obtained by multiplication of the enhancement factor to static concrete strength. The strength enhancement factors used in this study are shown in Fig. 1.

2.2 Steel reinforcement model

For the material model of steel reinforcement in concrete, dynamic and strength increasing factors are considered (LSTC 2006). The yield stress function of steel reinforcement based on the von Mises criterion is

$$\sigma_y = \beta[\sigma_0 + f_h(\varepsilon_{eff}^p)] \quad (5)$$

where, β is the variable for strain rate effect and is calculated using Eq. (6), which is based on Cowper and Symonds' model (Jones 1983). σ_0 is initial yield stress and $f_h(\varepsilon_{eff}^p)$ is hardening function, which can be expressed as Eq. (7) using plastic stiffness E_p and effective plastic strain

$\varepsilon_{eff}^p \cdot$

$$\beta = 1 + \left(\frac{\dot{\varepsilon}}{C} \right)^{(1/r)} \quad (6)$$

$$f_h(\varepsilon_{eff}^p) = E_p(\varepsilon_{eff}^p) \quad (7)$$

where, C and r are strain rate parameters. In this study, the strain rate effect is considered by defining the relationship between effective plastic strain and yield strength based on the experimental data. The relations between effective plastic strain and yield strength are shown in Fig. 2.

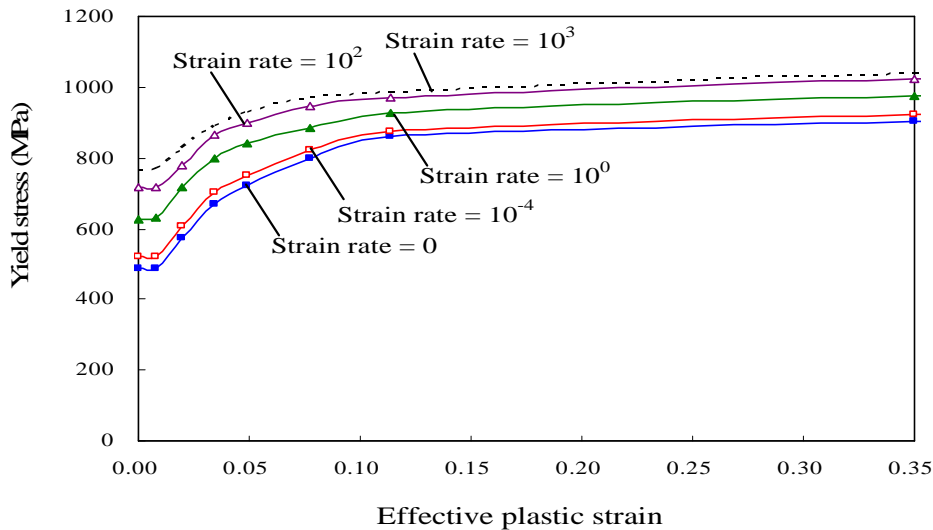


Fig. 2 Rate dependent relationship of effective plastic strain and yield stress for steel reinforcement

2.3 Rate dependent FRP failure model

The failure model of FRP in this study is based on progressive failure criteria of Hashin model (1980) and Chang and Chang's model (1987). The strain-rate effect on the material strengths is incorporated into failure model based on Park's model (2006). For tension failure, the fiber breakage criterion can be expressed as

$$e = \left(\frac{\sigma_{11}}{X_t} \right)^2 + \left(\frac{\tau_{12}}{SC_{12}} \right)^2 \text{ and } \left(\frac{\sigma_{11}}{X_t} \right)^2 \geq \left(\frac{\tau_{12}}{SC_{12}} \right)^2, \text{ for } \sigma_{11} > 0 \quad (8)$$

where, e is a failure index representing the combined effect of the normal and shear stresses; σ_{11} is normal stress; τ_{12} is shear stress; X_t is the tensile strength; SC is the in-plane shear strength. The

criterion states that fiber breakage occurs when the failure index is equal to or greater than unity, for cases where the effect of normal stress is greater than that of shear stress. For the compressive failure, the failure criterion can be expressed as

$$e = \left(\frac{\sigma_{11}}{X_c} \right)^2, \text{ for } \sigma_{11} < 0 \quad (9)$$

where, X_c is the compressive strength. The criterion states that fiber failure in compression is mainly due to the normal stress, because fiber buckling dominates the failure in compression. The strength values of failure criteria are dependent on strain-rate and can be expressed as follows.

$$X_t = f_1(\dot{\epsilon}), X_c = f_2(\dot{\epsilon}), Y_t = f_3(\dot{\epsilon}), Y_c = f_4(\dot{\epsilon}), SC_{12} = f_5(\dot{\epsilon}) \quad (10)$$

where, X is the longitudinal strength; Y is the transverse strength; SC_{12} is the in-plane shear strength; $\dot{\epsilon}$ is strain rate. Subscripts t and c represent tensile and compressive state. Specific functional forms $f(\dot{\epsilon})$ can be determined from experiment such as uniaxial and eccentric tension tests. Therefore, the uniaxial and eccentric tension tests should be carried out to predict the appropriate strain rate effect on the longitudinal and shear strength. Linear functions of material strength according to strain rates can be defined by Eqs. (11) to (13) (Al-Hassini and Kaddour 1998).

$$X = X^{static} + \zeta \dot{\epsilon}_{11} \text{ (MPa)} \quad (11)$$

$$Y = Y^{static} + \xi \dot{\epsilon}_{22} \text{ (MPa)} \quad (12)$$

$$SC_{12} = (SC_{12})^{static} + \kappa \dot{\epsilon}_{12} \text{ (MPa)} \quad (13)$$

where, ζ , ξ , κ are material constants. From Eqs. (11) to (13), the strain rate effect is simply related to the in-plane failure criteria of FRP failure model.

3. Blast analysis for FRP retrofitted RC slab

3.1 Descriptions of field blast test

In order to verify the proposed HFPB analysis method for RC structures under blast loading, a simulation analysis for the blast test conducted by Muszynski and Purcell (2003) is carried out. The detailed dimensions and conditions are summarized in Table 1 and Fig. 3. The main objective of this test is to evaluate the effectiveness of FRP retrofitting, so all the specimens are FRP retrofitted on their half wall and the rest half wall remains as bare wall. To consider this condition, the FRP on the RC wall in the test is also modeled as well as the RC wall structure.

The structures are retrofitted such that a half of the back side of the blast loaded face is attached with either CFRP or Kevlar/Glass hybrid fabric (K/G) sheet and the other half is non-retrofitted as a control. The retrofitting materials are applied to the interior walls. The front walls are subjected to blast loading due to external explosion of 830 kg of TNT from the 14.6 m stand-off distances.

Table 1 Properties of target structure and blast load characteristics

Compressive strength of concrete	Density of concrete	Steel yield strength
28 MPa	237 kg/m ³	415 MPa
Steel reinforcement	Explosive charge	Stand-off distance
9 mm rebar	TNT 830 kg	14.6 m

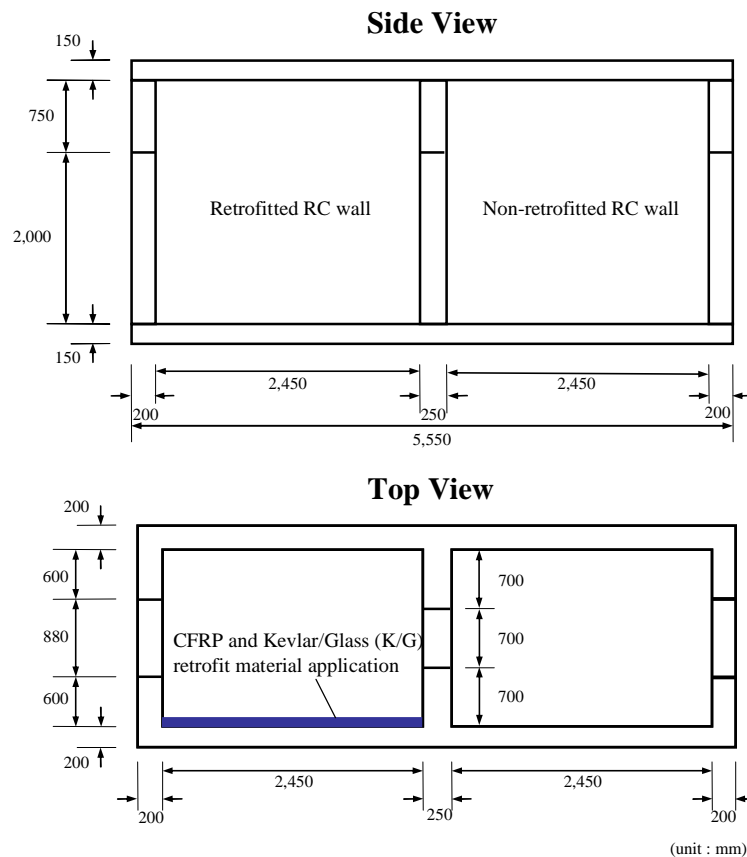


Fig. 3 Dimensions of tested RC wall

Table 2 properties of retrofit composite materials

Property	CFRP laminate	K/G hybrid knitted fabric
Fiber orientation	0/90/0	0/90
Thickness (mm)	0.5	0.5
Tensile strength (MPa)	2,270	223
Modulus (GPa)	13.8	11

At this distance, the non-retrofitted RC walls are expected to receive moderate damage with significant residual displacement and some spalling from interior surface. On the other hand, the retrofitted walls are expected to have less residual displacement and no spalling from interior surface. The material properties for both retrofit composite materials are described in Table 2.

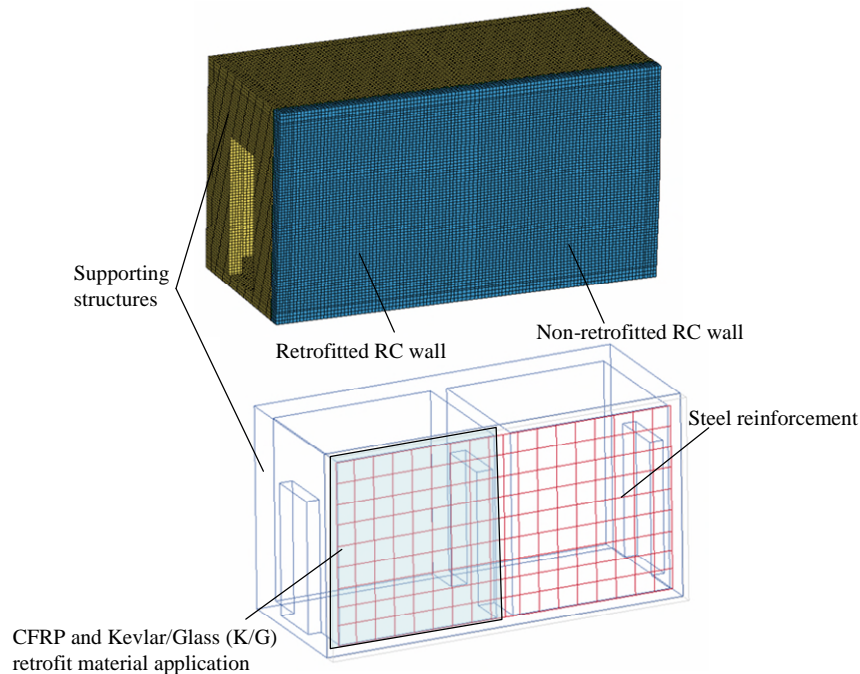


Fig. 4 FE Model of target structure

3.2 Finite element models

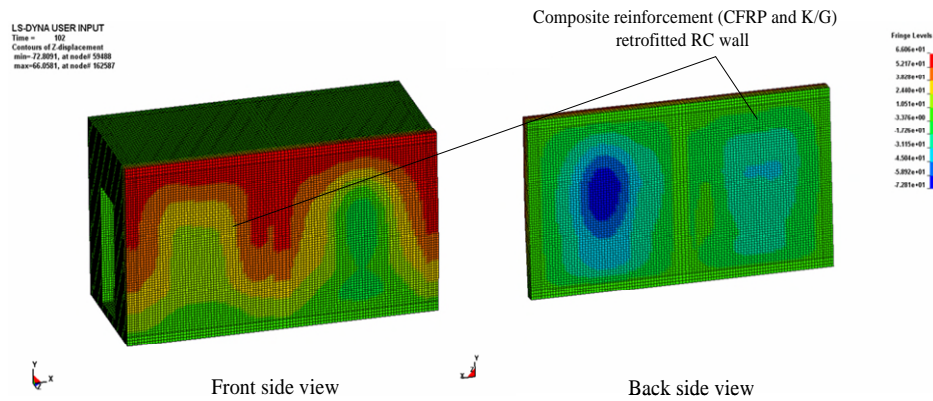
Solid and beam elements with rate dependent material models are used for concrete and reinforcing steels, respectively. For the FRP sheets modeling, shell element with rate independent and dependent failure models are adopted to incorporate FRP rate effect on the global structural behavior. The shell elements of FRP are attached to the solid elements of concrete with contact interface element. The shell elements are placed at a distance of half-thickness of FRP sheet from the concrete surface. This virtual thickness offset is used to simulate the attachment of FRP to the concrete in the analysis. For the determination of element size, noise analyses for the different element sizes were conducted and 2.5% of specimen length was determined as an optimum element size considering the computing time and the reliability. The FE modeling including concrete, reinforcing steel and FRP sheet of the retrofitted slab is schematically shown in Fig. 4.

3.3 Material models

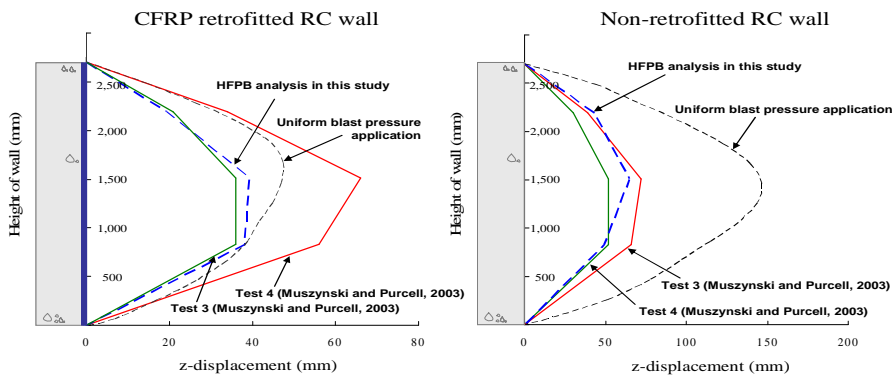
Solid and beam elements with rate dependent material models are used for concrete and reinforcing steels, respectively. For the FRP sheets modeling, shell element with rate independent and dependent failure models are adopted to incorporate FRP rate effect on the global structural behavior. The shell elements

3.4 Analysis results and discussions

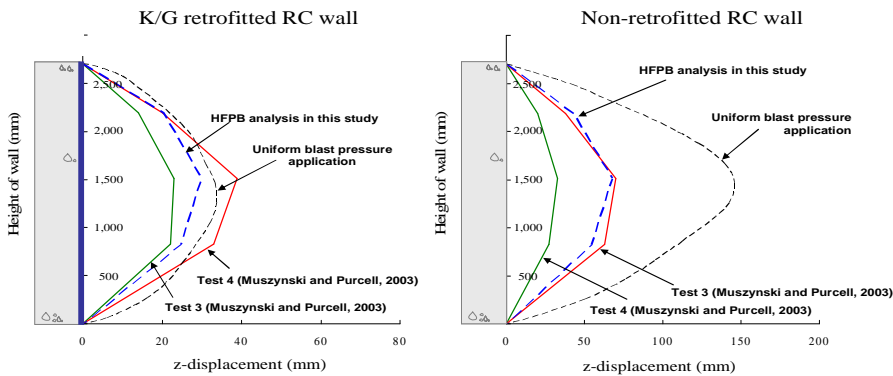
The analysis for the test specimen in accordance with the proposed analysis method was carried



(a) Displacement distribution contour



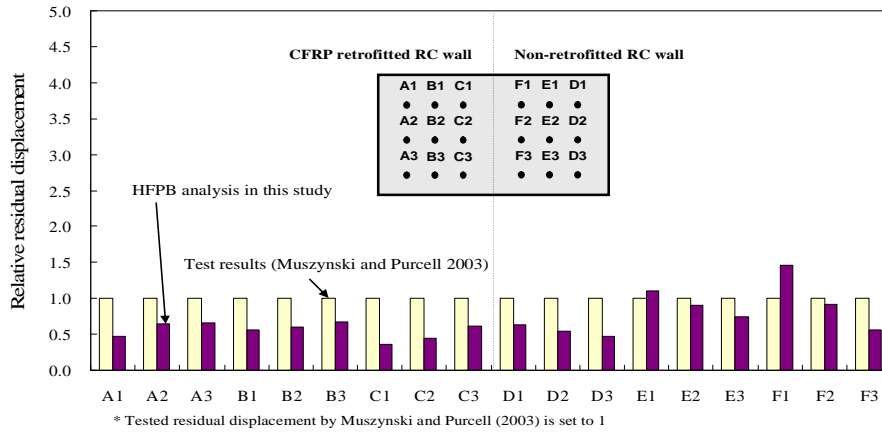
(b) Residual displacement comparison in case of CFRP application



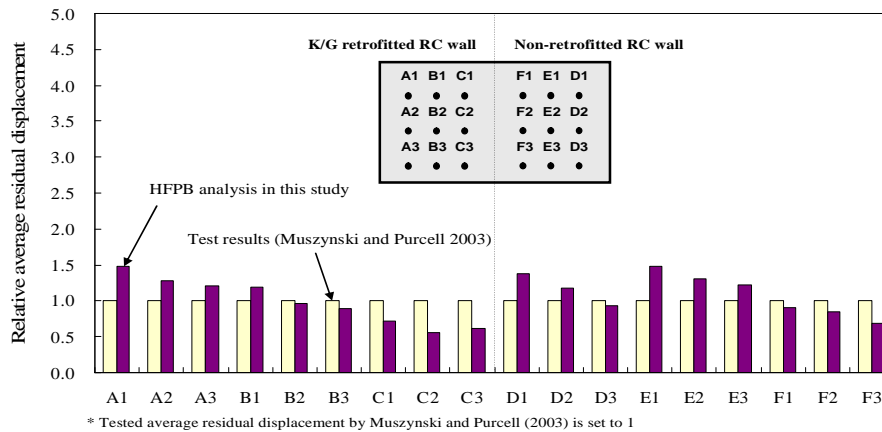
(c) Residual displacement comparison in case of K/G application

Fig. 5 Comparison of residual displacements

out. The analysis results are shown in Fig. 5. The maximum displacement of the bare wall from the analysis is greater than the average maximum value of the test by approximately 24%. In the case of CFRP retrofitting, the maximum residual displacement from the analysis is smaller than the average maximum value of the test by approximately 22%. In this case, both stress and strain of CFRP exceed its ultimate strength and strain limit. This result is indicated by the failure and



(a) CFRP retrofitted RC wall



(b) K/G retrofitted RC wall

Fig. 6 Relative residual displacements of RC wall

delamination of CFRP in the test. On the other hand, the maximum residual displacement from the analysis is smaller than the average maximum value of the test by about 3.6% in the case of K/G retrofitting. In both cases of analysis and test, the consistent trend for retrofitting effect is shown. This indicates that the analysis with the proposed HFPB analysis method can simulate the behavior of the RC wall realistically.

On the other hand, the relative residual displacements of the measuring points on the wall are shown in Fig. 6. Overall relative displacements from analysis on measuring points have little differences with the results of test. This indicates that the displacements distribution of the analysis agrees well with that of test. Especially, the trend of FRP retrofitting performance from the analysis results coincides with the experimental trend. However, in the case of CFRP retrofitting, the analysis results are underestimated than experimental results. This could be induced from the material failure and spalling due to the brittle material properties of CFRP. In addition, the relative displacements on the point of center area are evaluated to be smaller than that of test and this can be considered as the noise effect due to the interaction between bare wall and retrofitted wall.

4. Conclusions

The blast analysis methodology for the evaluation of FRP retrofitting effectiveness is presented. Rate dependent material models for concrete, steel and FRP are adopted for the numerical analysis technique. The blast analysis is carried out for FRP retrofitted RC wall and analysis results are compared with the previously reported experimental results. For the rate dependent material models, the enhanced failure criteria are defined. Different increasing factors are applied to consider the material characteristics of concrete, steel and FRP, respectively. In the comparative study, the FRP retrofitting effectiveness is evaluated by using different FRP types: CFRP and K/G. The residual displacement distributions for each case are analyzed in the respects of global structural behavior and retrofitting sufficiency. The numerical analysis results are verified with experimental data which have been measured by previous researchers. Even though the experimental data varies with ranges, the analysis results of overall displacement history and FRP failure correspond with experimental results. The presented blast analysis procedure is confirmed to be used for the evaluation of FRP effectiveness in the blast retrofitting design. Further experiments on the strain-rate effect according to the various types and layers of FRP are needed to build more accurate model and retrofitting design procedure for RC structure under blast loading. Also, further researches on the dynamic interfacial behavior between FRP and concrete are required.

Acknowledgments

The research described in this paper was financially supported by NRF, Republic of Korea (NRF-2013R1A1A2060227).

References

- Al-Hassini, S.T.S. and Kaddour, A.S. (1998), "Strain rate effect on GFRP, KFRP and CFRP composite laminates", *Key Eng. Mater.*, **141-143**(2), 427-452.
- ASCE (1999), "Structural design for physical security", State of the Practice.
- Biggs, J.M. (1964), *Introduction to Structural Dynamics*, McGraw-Hill, New York.
- Brena, S.F. and McGuirk, G.N. (2013), "Advances on the behavior characterization of FRP-anchored carbon fiber-reinforced polymer (CFRP) sheets used to strengthen concrete elements", *Int. J. Concrete Struct. Mater.*, **7**(1), 3-16.
- Buchan, P.A. and Chen, J.F. (2007), "Blast resistance of FRP composite and polymer strengthened concrete and masonry structures: A state-of-the-art review", *Compos. Part B: Eng.*, **38**(5-6), 509-522.
- Chang, F.K. and Chang, K.Y. (1987), "A progressive damage model for laminated composite containing stress concentration", *J. Compos. Mater.*, **21**(9), 834-855.
- Chen, W.F. (1982), *Plasticity in Reinforced Concrete*, McGraw Hill, New York.
- Grelle, S.V. and Sneed, L.H. (2013), "Review of anchorage system for externally bonded FRP laminates", *Int. J. Concrete Struct. Mater.*, **7**(1), 17-33.
- Hashin, Z. (1980), "Failure criteria for unidirectional fiber composite", *J. Appl. Mech.*, **47**(2), 329-334.
- Jerome, D.M. and Ross, C.A. (1997), "Simulation of the dynamic response of concrete beams externally reinforced with carbon-fiber reinforced plastic", *Comput. Struct.*, **64**(5-6), 1129-1153.
- Jones, N. (1983), *Structural aspects of ship collisions*, Ed. Jones N, Wierzbicki T, Structural Crashworthiness, Butterworths, London.

- LSTC (2006), LS-DYNA Keyword User's Manual Version 9.71, Livermore Software Technology Corporation.
- Malvar, L.J., Morrill, K.B. and Crawford, J.E. (2004), "Numerical modeling of concrete confined by fiber-reinforced composites", *J. Compos. Constr.*, **8**(4), 315-322.
- Muszynski, L.C. and Purcell, M.R. (2003), "Composite reinforcement to strengthen existing concrete structures against air blast", *J. Compos. Constr.*, **7**(2), 93-97.
- Park, H., Lee, K., Lee, S.W. and Kim, K. (2006), "Dynamic analysis of nonlinear composite structures under pressure wave loading", *J. Compos. Mater.*, **40**(15), 1361-1383.
- Razaqpur, A.G., Tolba, A. and Contestabile, E. (2007), "Blast loading response of reinforced concrete panels reinforced with externally bonded GFRP laminates", *Compos. Part B: Eng.*, **38**(5-6), 535-546.
- Silva, P.F. and Lu, B. (2007), "Improving the blast resistance capacity of RC slabs with innovative composite materials", *Compos. Part B: Eng.*, **38**(5), 523-534.
- White, T.W., Soudki, K.A. and Erki, M.A. (2001), "Response of RC beams strengthened with CFRP laminates and subjected to a high rate loading", *J. Compos. Constr.*, **5**(3), 153-162.